Planetary and Space Science 113-114 (2015) 292–297

Contents lists available at ScienceDirect

Planetary and Space Science

journal homepage: www.elsevier.com/locate/pss

Ground-based IR observation of oxygen isotope ratios in Venus's atmosphere

N. Iwagami [a,*,1], G.L. Hashimoto [b,1], S. Ohtsuki [c,1], S. Takagi [a,1], S. Robert [d,1]

[a] Department of Earth and Planetary Science, University of Tokyo, Bunkyo-ku, Tokyo 113-0033, Japan
[b] Department of Earth Sciences, Okayama University, Tsushima-naka, Okayama 700-8530, Japan
[c] School of Commerce, Senshu University, Higashimita, Tama-ku, Kawasaki 214-8580, Japan
[d] Belgian Institute of Space Aeronomy, 3 Av. Circulaire, B-1180 Brussels, Belgium

ARTICLE INFO

Article history:
Received 6 March 2014
Received in revised form
28 July 2014
Accepted 6 October 2014
Available online 12 November 2014

keywords:
Oxygen isotope
Venus atmosphere
Ground-based
IR spectroscopy

ABSTRACT

The oxygen isotope ratios $^{17}O/^{16}O$ and $^{18}O/^{16}O$ in Venus's atmosphere were measured simultaneously by ground-based IR spectroscopy. The CO_2 absorption lines in the 2648 cm^{-1} (for $^{17}O/^{18}O$) and 4582 cm^{-1} (for $^{18}O/^{16}O$) regions were observed using the IRTF/CSHELL spectrometer. The deviations of the isotope fractions are found to be $\delta^{17}O = +92 \pm 158‰$ and $\delta^{18}O = -42 \pm 85‰$ as compared to the terrestrial standard (HITRAN 2012) where the uncertainties include both random and systematic errors. Such combination agrees with the Earth–Moon fractionation line within the errors. This is consistent to the fact that the proto-Venus matter was also well mixed with the proto-Earth–Moon matter.

1. Introduction

The isotope ratios in the planetary atmosphere provide important information in studying the origin and the evolution of the planets. In case of Venus, the D/H (deuterium to hydrogen) ratio has been investigated extensively because it is more than 100 times larger than the terrestrial ratio (*e.g.* Donahue et al., 1997) telling something important about the early Venusian history. In such a way, other isotope ratios such as $^{17}O/^{16}O$ and $^{18}O/^{16}O$ may also be expected to tell us something interesting about the history of the planets and the solar system.

The deviation in proportion of an isotope that is in a sample is expressed as

$$\delta X = [(R_{sample}/R_{standard}) - 1] \times 1000 \quad (1)$$

where X represents the isotope of interest, δX is given in permil (‰) and R represents the ratio of the isotope of interest to its natural form (*e.g.* $^{18}O/^{16}O$). In the present paper, we adopt ratios used in HITRAN 2012 (Rothman et al., 2013) as the standard because they are used whole through the present paper; however, the values are a little different from those of VSMOW (Vienna Standard Mean Ocean Water: *e.g.* Coplen et al., 2002). According to HITRAN 2012, we have $R_{standard}$ ($^{18}O/^{16}O$) = 0.0020052 and $R_{standard}$ ($^{17}O/^{16}O$) = 0.0003728. Those ratios may be calculated from the CO_2 fractional abundances of HITRAN listed in Table 1 as the former = 0.003947/0.9842/2 and the latter = 0.0007339/0.9842/2. The former is exactly the same as the VSMOW value through 5 digits, however the latter is smaller than the VSMOW value of 0.0003799 by 19‰ which may not be ignored.

Isotope ratios can be plotted in function of one another, as shown in Fig. 1, adapted from Scott (2001). The correlation plot of the oxygen isotope ratios $^{17}O/^{16}O$ and $^{18}O/^{16}O$ in the Earth–Moon rocks shows a clear linear relation with a slope of 0.5. On Fig. 1, $\delta^{17}O$ and $\delta^{18}O$ represent the deviations of the isotope fractions from the VSMOW standard ratios in units of permil (‰). The slope of 0.5 comes from the equi-difference between the mass numbers (16, 17 and 18). As shown on Fig. 1, the correlation lines vary from one planet to another. For example, the correlation line for Mars meteorites is above that for Earth–Moon by 0.5‰. This fact indicates that the proto-Earth-Mars matter in the proto-solar nebula was well mixed, and that a systematic difference of 0.5‰ between Earth–Moon and Mars was kept on the other hand. On each body, the oxygen isotopes were separated according to their masses when the rocks formed. Studying isotope ratios may provide various insights into the origin and evolution of the planets. Recently, McKeegan et al. (2011) found that the correlation line in the captured solar wind particle shows a slope of 1 not 0.5; a new riddle has been discovered. Thiemens (1999) showed that such plots for the terrestrial stratospheric and mesospheric CO_2 do not align on the Earth–Moon line, but come to the upper

* Corresponding author.
E-mail address: iwagami@eps.s.u-tokyo.ac.jp (N. Iwagami).
[1] Visiting astronomers at the Infrared Telescope Facility.

http://dx.doi.org/10.1016/j.pss.2014.10.004
0032-0633/

Table 1
CO_2 isotope fractional abundances in the terrestrial atmosphere (HITRAN 2012).

$^{16}O\ ^{12}C^{16}O$ (626)	0.9842
$^{16}O\ ^{13}C^{16}O$ (636)	0.01106
$^{16}O\ ^{12}C^{18}O$ (628)	0.003947
$^{16}O\ ^{12}C^{17}O$ (627)	0.0007339

626, 636, 628 and 627 are abbreviated code for isotopologues.

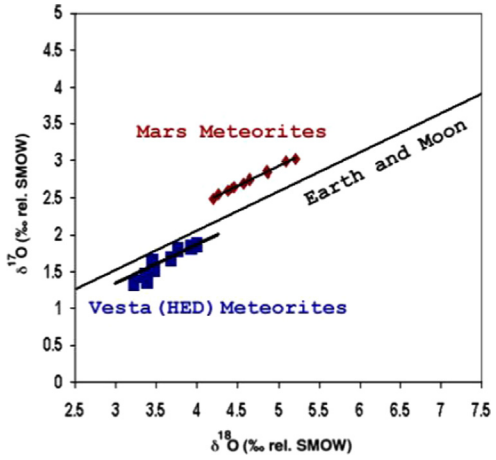

Fig. 1. Correlation plot of $\delta^{17}O$ and $\delta^{18}O$ in Earth–Moon rocks and meteorites from Mars and asteroid Vesta. $\delta^{17}O$ and $\delta^{18}O$ represent deviations of the isotope fractions from the terrestrial standard SMOW (standard mean ocean water) in units of permil (‰). The slope of 0.5 comes from the equi-difference between the mass numbers (16, 17 and 18). (Figure after Scott (2001)).

side probably due to exchange reaction with $O(^1D)$ produced by the solar UV. The Pioneer Venus mass spectrometer of Hoffman et al. (1980) gave the result $^{16}O/^{18}O = 500 \pm 25$ (equivalent to $\delta^{18}O = -3 \pm 50‰$). The ratio $^{16}O/^{18}O$ has also been measured spectroscopically in the 10 μm region (Bezard et al., 1987) to be 500 ± 80 (equivalent to $\delta^{18}O = -3 \pm 160‰$) in agreement with the terrestrial ratios within the error. However, as seen in the figure such correlation between $\delta^{17}O$ and $\delta^{18}O$ in Venus has never been investigated.

The purpose of the present work is to show the isotope ratios $^{17}O/^{16}O$ and $^{18}O/^{16}O$ in Venus's atmosphere measured simultaneously, and to provide information about the mixing history of the early solar nebula.

2. Observation

The observations were carried out at IRTF (Infrared Telescope Facility, Hawaii) with the CSHELL spectrometer (Greene et al., 1993) in July 2012. The observation conditions are listed in Table 2. CSHELL is an Echelle grating spectrometer with a nominal resolution of 42,000.

There are some requirements in selecting the CO_2 lines and the wavenumber regions to be used. They are as follows:

(1) Less solar and terrestrial interferences,
(2) Moderate line intensities (not too strong to saturate, and not too weak to be overcome by noise),
(3) Two kinds of isotope signatures seen in one small wavenumber region to simplify analysis, and
(4) Small lower state energy E'' for small temperature dependence.

However, all the above requirements usually cannot be entirely satisfied as will be discussed in a latter section. The requirement

Table 2
Observation parameters.

Date	11–15 July 2012
Time	06–14 h (HST*)
Object	Dayside reflected sunlight
Site height	4200 m
Telescope diameter	3.0 m
Typical seeing	1.0"
Actual resolution	38,500
Slit width	0.5"
Pixel pitch	0.2"
Venus diameter	38.2–35.8"
Phase angle	118.2–112.9°
Doppler speed	12.4–12.9 km s^{-1}

* HST(Hawaiian Standard Time)=UT-10h.

3 provides an advantage that interference due to wavenumber dependence of the cloud parameter may be canceled out. Measurements in two spectral regions are needed because the two isotope ratios $^{17}O/^{16}O$ and $^{18}O/^{16}O$ must be measured. We chose to measure the spectral regions 2645–2651 cm^{-1} and 4577–4587 cm^{-1}. The first one, centered around 2648 cm^{-1} has been used because both $^{16}O^{12}C^{17}O$ (627) and $^{16}O^{12}C^{18}O$ (628) lines are dominant (see Fig. 3(a)). It enabled us to determine the 627/628 (not 627/626) ratio. The second region, centered around 4582 cm^{-1} contains both $^{16}O^{12}C^{18}O$ (628) and $^{16}O^{12}C^{16}O$ (626) lines (see Fig. 3(b)) and is used to find the 628/626 ratio. By combining information from both regions, the ratios $^{17}O/^{16}O$ and $^{18}O/^{16}O$ may be quantified.

The slit of 30" in length was aligned in the north–south direction of Venus fixed in the central brightest area of the disk parallel to the terminator. A two-dimensional InSb detector (256 × 256 operated at 30 K) is used to obtain the spectroscopic and latitudinal information simultaneously. The 24" central part of the 30" slit is used so that the measured latitude range is ±41° (=$\sin^{-1}$(12"/Venus radius 18.2")). However, latitudinal information is averaged out, and is not used in the present work. The single exposure durations were 30 s and 3 s for the 2648 and 4582 cm^{-1} regions, respectively. The total numbers of spectra co-added are 50,600 and 73,200, respectively (each spectro-image consists of 120 latitudinal components).

The widths of the instrumental functions were estimated by measuring the FWHM (full width at a half maximum) of the emission lines of Ar and Kr lamps used for the wavelength calibration. They were found to be 0.068 cm^{-1} and 0.120 cm^{-1} for the 2648 $cm^{-1}$and 4582 cm^{-1} regions, respectively. This means actual resolutions of 38,900 and 38,200, respectively.

Fig. 2(a) and (b) shows the averaged spectra on each day. In the 2648 cm^{-1} region, measurements were successful on 11th, 12th 14th and 15th July obtaining 6000, 6000, 21,800 and 16,800 spectra, respectively. In the 4582 cm^{-1} region, measurements were successful on 12th, 13th and 15th July obtaining 6000, 51,800 and 15,400 spectra, respectively. As seen in the figures these averaged spectra seem to reach signal-to-noise (S/N) ratios of 3000 or more. Since they have not yet been corrected for terrestrial absorption, some disturbance due to terrestrial H_2O or CH_4 is apparent such as seen at 4580 cm^{-1}.

3. Data analysis

Fig. 3(a) and (b) demonstrates the analysis procedures.

In Fig. 3(a) the 2648 cm^{-1} region is shown for the Doppler shift of −0.11 cm^{-1} with an instrumental width of 0.068 cm^{-1}. Plotted together are observed average spectrum (gray), solar spectrum (red), terrestrial transmission (blue), ratio spectrum (=observed/solar/terrestrial: black) and calculated Venus reflected spectra

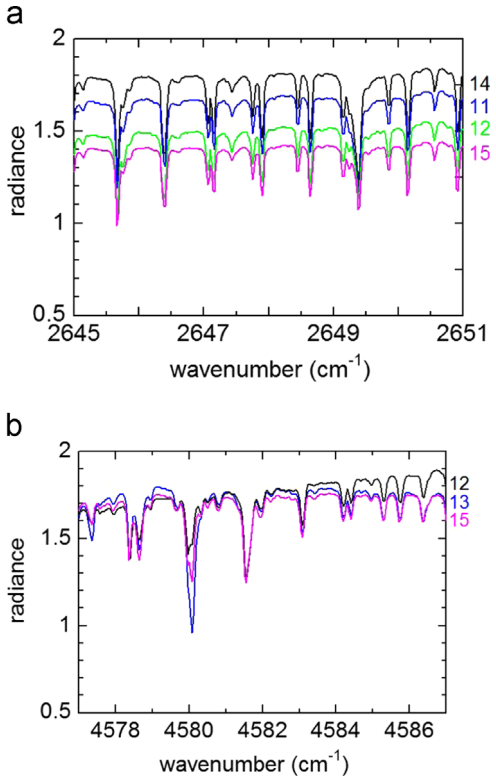

Fig. 2. (a) Averaged spectra in the 2648 cm^{-1} region measured on 11th (blue), 12th (green), 14th (black) and 15th (purple) July 2012. (b) Averaged spectra in the 4582 cm^{-1} region measured on 12th (black), 13th (blue) and 15th (purple) July 2012. Terrestrial H_2O absorption is seen at 4580 cm^{-1}. (For interpretation of the references to color in this figure legend, the reader is referred to the web version of this article.)

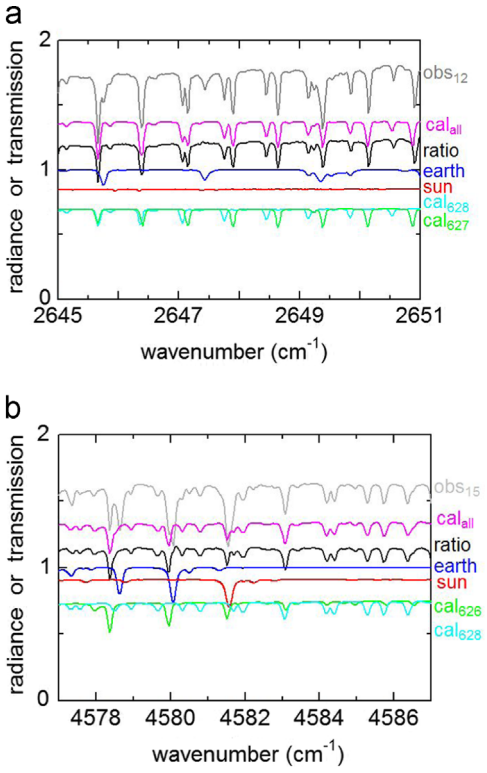

Fig. 3. (a) Demonstration of analysis procedure in the 2648 cm^{-1} region for the Doppler shift of -0.11 cm^{-1} with and instrumental width of 0.068 cm^{-1}. Plotted together are observed average spectrum (gray), solar spectrum (red), terrestrial transmission (blue), ratio spectrum (=observed/solar/terrestrial: black) and calculated Venus reflected spectra including all species (purple), only 627 CO_2 (green) and only 628 CO_2 (sky blue). The isotope ratio $^{17}O/^{18}O$ is determined by fitting the calculated spectrum (cal_{all}) to the observed one (ratio). Most of the curves are shifted vertically by a certain amount for clearness. (b) Same as for Fig. 3(a) but in the 4582 cm^{-1} region for the Doppler shift of -0.19 cm^{-1} with an instrumental width of 0.120 cm^{-1}. The calculated Venus reflected spectra including only 628 CO_2 (sky blue) and only 626 CO_2 (green) are also plotted. (For interpretation of the references to color in this figure legend, the reader is referred to the web version of this article.)

including all species (purple), only $^{16}O^{12}C^{17}O$ (627: green) and only $^{16}O^{12}C^{18}O$ (628: sky blue).

The solar spectrum is taken from a solar line atlas (Livingston and Wallace, 1991). The terrestrial transmission is calculated by a line-by-line method based on the HITRAN 2012 molecular database (Rothman et al., 2013) and MSIS-E90 terrestrial model atmosphere (Picone et al., 2002). The Venus dayside spectra are from HITRAN 2012, VIRA 1985 model atmosphere (Seiff et al., 1985) and the reference cloud model of Takagi and Iwagami (2011) based on the descending probes of the Veneras 9–14 and Pioneer Venus large probes. In the Venus calculation, scattering by the cloud particles is taken into account by using a plane-parallel radiative transfer code RSTAR (Nakajima and Tanaka, 1986, 1988). The Voigt profile (Humlicek, 1982) is applied for the line shape. The mixing ratio profiles of Venusian minor constituents are taken from Pollack et al. (1993). The continuum absorption due to CO_2 and H_2O, and the sub-Lorenzian line shape for CO_2 are taken into account in the same way as in Pollack et al. (1993).

In this wavenumber region, most Venus absorption lines are due to 627 and 628 (not 626) with just a little contribution from HDO. The terrestrial absorptions are due to CH_4 and H_2O. Fortunately, little disturbance due to solar lines is present. The correction for the terrestrial absorptions is performed by adjusting the calculated to the observed spectra to minimize the RMS (root mean square) deviation around the terrestrial lines. It is seen in the figure that the ratio spectrum (black) is well reproduced by the calculated spectrum (purple). Two pairs of closely-located 627 and 628 lines at around 2647.8 and 2648.5 cm^{-1} in Fig. 3(a) are used to quantify the isotope ratio.

In Fig. 3(b), the 4582 cm^{-1} region is shown for the Doppler shift of -0.19 cm^{-1} with an instrumental width of 0.120 cm^{-1}. In this figure, calculated Venus reflected spectra including only $^{16}O^{12}C^{18}O$ (628: sky blue) and only $^{16}O^{12}C^{16}O$ (626: green) are also plotted. In this wavenumber region, all the Venus absorption lines seen in the figure are due to 628 and 626. The terrestrial lines are due to CH_4 and H_2O. Less fortunately than in the 2648 cm^{-1} region, there are some solar and terrestrial absorption lines disturbing the quantification. As a closely located pair of 628 and 626 absorption lines could not be found in this region, two spectral regions separated by 6 cm^{-1} are used. The 4577.8–4580.6 cm^{-1} region is used for the 626 lines, and the 4583.8–4586.8 cm^{-1} region for the 628 lines.

In Fig. 4(a) and (b), the fitting procedure to quantify the isotope ratios is demonstrated. The procedure consists of the following three steps: (1) high-pass filtering, (2) cloud height optimization and (3) isotope ratio optimization.

Step (1): The spectrum in Fig. 4(a) noted as hpObs (blue) is calculated from the ratio spectrum in Fig. 3(a) by removing the trend with a high-pass filter with a width of 0.8 cm^{-1}, and the one noted as hpCal (purple) is from the calculated Venus spectrum cal_{all} in Fig. 3(a) by removing the trend with the same filter. These two spectra appear to overlap each other almost completely. The high-pass filtering is to calculate the ratio of the initial spectrum to the low-pass filtered spectrum. Also in the figure, the residual (=hpObs-hpCal: black and gray) is shown. Only the black portion is used to evaluate the RMS

(root mean square) deviation; this is to reduce interferences from the solar and terrestrial structures. The same procedure is taken in the 4582 cm^{-1} region with a high-pass width of 1.6 cm^{-1} as shown in Fig. 4(b). The hpCals in Fig. 4(a) and (b) are the final ones after optimization for the cloud height and the isotope ratios.

Step (2): The initial Venus spectrum is calculated for the standard cloud condition (Takagi and Iwagami, 2011) and the standard isotope ratio (HITRAN 2012). The high-pass component of such initial calculated spectrum hpCal usually shows different amplitude from that of hpObs. The optimum cloud height is determined by minimizing its RMS deviation from hpObs by adjusting the cloud height used for calculating hpCal. In the cloud model used here (Takagi and Iwagami, 2011), the height level for unit optical depth (at 920 nm) appears at 70 km (0.34 by mode 1 and 0.66 by mode 2). The optimized cloud heights are found to be higher than the standard by 3.53, 2.77, 2.78 and 2.98 km on 11th, 12th, 14th and 15th July, respectively, in the 2648 cm^{-1} region. They are 3.09, 2.39 and 2.56 km higher than the standard on 12th, 13th and 15th of July, respectively, in the 4582 cm^{-1} region.

Step (3): In the 2648 cm^{-1} region, the 627/628 ratio may be obtained by minimizing the RMS deviation of the spectrum optimized for cloud height in Step (2) from hpObs by changing the 627/628 ratio. The optimized ratios are found to be larger than the terrestrial standard by factors of 1.2057, 1.0995, 1.1105 and 1.1172 on 11th, 12th, 14th and 15th July, respectively; the average is 1.1332 ± 0.0488. It indicates an excess of 133.2 ± 48.8‰. The same procedure is applied for the 4582 cm^{-1} region for 628/626 ratio as demonstrated in Fig. 4(b). In this case, two regions 4577.8–4580.6 cm^{-1} and 4583.8–4586.8 cm^{-1} are used for 626 and 628 quantification, respectively. Those wavenumber regions are selected because of less interference due to terrestrial and solar structures. The optimized 628/626 ratios are found to be 0.96883, 0.94798 and 0.95877 times of the terrestrial standard on 12th, 13th and 15th of July, respectively; the average is 0.95853 ± 0.01043. It indicates an deficit of 41.5 ± 10.4‰ as compared to the terrestrial standard ratio.

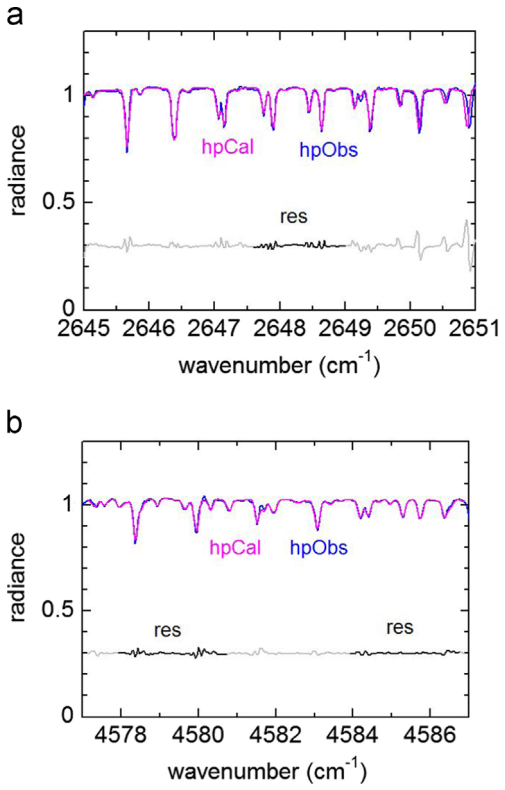

Fig. 4. (a) Demonstration of analysis procedure in the 2648 cm^{-1} region. Plotted together are observed (blue) and calculated (purple) spectra after high-pass procedure and the residual (black and gray: shifted by 0.3). Only the black portion of residual is used to evaluate the RMS error. Beyond 2650 cm^{-1}, a systematic wavenumber error is seen. This is due probably to a wrong calibration procedure, and the region is not used for optimization. (b) Same as in Fig. 4(a), but in the 4582 cm^{-1} region. Two black portions of the residual are used to evaluate the RMS error. (For interpretation of the references to color in this figure legend, the reader is referred to the web version of this article.)

Summarizing the above information, $\delta^{18}O = -42 \pm 10$‰ and $\delta^{17}O = +92 \pm 50$‰ where the errors include those from day-to-day spread only. The value 92 comes from 133.2–41.5 = 91.7 and 50 from $(10.4^2+48.8^2)^{1/2}=49.9$.

Another random error source, uncertainty in temperature, must also be taken into account. In the present paper, VIRA1985 model (Seiff et al., 1985) is adopted, and deviation from that causes error in the isotope ratio through changes in the line intensities. The line intensity changes in proportion to

$$r(T, E'') = (T_0/T)\ \exp\ (1.44E''(1/T_0 - 1/T)), \quad (2)$$

where T is temperature in K, T_0 is the reference temperature 296 K and E'' is lower state energy in unites of cm^{-1}. The values of E'' for representative lines are listed in Table 3; in case of the 2648 cm^{-1} region, E''s are 830.0 and 34.1 cm^{-1}, and in the 4582 cm^{-1} region, they are 1013.8 and 106.1 cm^{-1}. According to VIRA1985 low latitude model, temperature at 70 km is 229.8 K, and that in the 45° model is 228.2 K differing only 1.6 K. Since the measurements extend up to ±41°, temperature uncertainty of 3 K (for example, 230 to 233 K) seems to be enough for consideration. For example, r (233,830)/r (230,830) = 1.05538, r (233,34.1)/r (230,34.1) = 0.98984, and 1.05538/0.98984 = 1.06621; this means random error of 66‰ may be expected for the 627/628 ratio in case of 3 K uncertainty. In the same way, that in the 628/626 ratio is found to be 76‰.

Summarizing the above information, $\delta^{18}O = -42 \pm 77$‰ and $\delta^{17}O = +92 \pm 113$‰ where the errors include random error only. The value 77 comes from $(10.4^2+76.1^2)^{1/2}=76.8$, and 113 from $(76.8^2+48.8^2+66.2^2)^{1/2}=112.5$.

In addition to random errors, systematic errors must be taken into account. According to HITRAN 2012, the line intensities uncertainties are larger than 200‰. These values are larger than the ones presented in HITRAN 2008, and their origins have been investigated. From private communications with I. Gordon and V. Perevalov, it appears that the 200‰ value is a conservative number corresponding to the root-mean square of the global fits

Table 3
Representative CO_2 line parameters (HITRAN 2012 and Perevalov, private communication 2014).

Isotope	Wavenumber (cm^{-1})	Intensity (cm)	Intensity uncertainty (‰)	Lower state energy (cm^{-1})	Vibrational band	Rotational assignment
628	2648.56	3.316e−26	30	830.0	20002-00001	R47
627	2648.75	1.175e−26	100	34.1	20002-00001	R9
626	4578.56	1.145e−26	20	106.1	31103-00001	P16
628	4585.92	9.648e−27	30	1013.8	00021-00001	P52

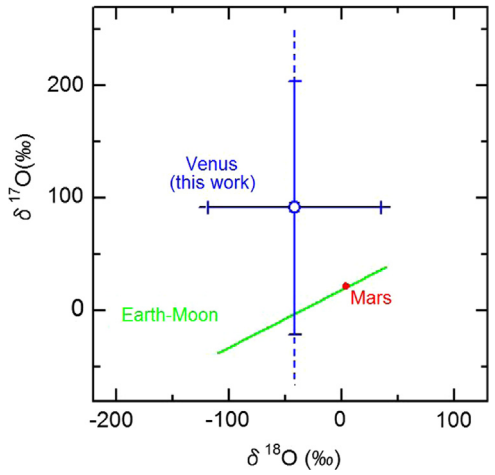

Fig. 5. Correlation plot of $\delta^{17}O$ and $\delta^{18}O$ for Earth–Moon rocks (green), Mars meteorites (red) and Venus's atmosphere (blue: present work) based on the standard isotope ratio of HITRAN 2012. The error bars are for random error (blue solid lines) and for systematic errors (blue dotted lines). Earth–Moon and Mars data are taken from McKeegan et al. (2011) and shifted by +19‰ for HTRAN-VSMOW difference. (For interpretation of the references to color in this figure legend, the reader is referred to the web version of this article.)

of positions and intensities, performed as described in Borkov et al. (2014). Realistic uncertainties of the line intensities in each band of interest were provided by V. Perevalov (private communication 2014). They range from 20–100‰ and are given in Table 3. They are of the same order of magnitude as the 100‰ of random error.

Summarizing the above information, $\delta^{18}O=-42\pm85$‰ and $\delta^{17}O=+92\pm158$‰ where the errors include both random and systematic errors, and they are plotted in Fig. 5. The value 85 comes from $(76.8^2+20^2+30^2)^{1/2}=84.8$, and 158 from $(84.8^2+82.2^2+30^2+100^2)^{1/2}=157.6$.

4. Discussion

The isotope ratios obtained using the method described earlier are $\delta^{17}O=+92\pm158$‰ and $\delta^{18}O=-42\pm85$‰. These results are plotted on Fig. 5 among the Earth–Moon and Mars fractionation lines. This figure is similar to Fig. 1 but showing a larger area. Note that the Earth–Moon line and the Mars points are shifted upward by 19‰ because of the difference between the standards of HITRAN and VSMOW as noted in a previous section. The point of the present result comes to the upper side of the Earth–Moon fractionation line as is the Martian line, and the region of errors overlaps with a part of the Earth–Moon line. The correlation of the isotope ratios found in Venus's atmosphere agrees with the Earth–Moon and the Mars fractionation lines within errors. This means that the Earth-like planets, Earth, Mars as well as Venus have been produced from a well-mixed proto-solar nebula. It must also be noted that such three isotope plot for CO_2 in the terrestrial stratosphere and mesosphere appears above the Earth–Moon line by 5–15‰ showing a slope of 1 not 0.5 (Thiemens, 1999). This is explained as an effect due to an exchange reaction of CO_2 with exited oxygen atom $O(^1D)$ produced by the solar UV as $^{17}O(^1D)+{}^{16}O^{12}C^{16}O\rightarrow{}^{16}O(^3P)+{}^{16}O^{12}C^{17}O$ where heavier product is favored than the lighter $^{16}O^{12}C^{16}O$. In the terrestrial troposphere under the condition of no solar UV, the three isotope plot comes on the Earth–Moon line (Thiemens, 1999). The sampling height for the present measurement is estimated to be about 70 km at the cloud top where the solar UV is also available to produce $O(^1D)$, and a similar effect is expected for the Venusian three line plot to appear above the fractionation line for Venus tropospheric CO_2 and rocks.

5. Conclusion

First simultaneous measurement of deviations of the isotope fractions $\delta^{17}O$ and $\delta^{18}O$ in Venus's atmosphere has been done. They are found to be $+92\pm158$‰ and -42 ± 85‰, respectively, as compared to the terrestrial standard of HITRAN 2012. This combination agrees with the Earth–Moon fractionation line within the errors. It seems to indicate that the proto-Venus matter was also well mixed with the proto-Earth–Mars matter. However, the total of random and systematic errors in the present work exceeds 100‰.

Acknowledgments

The authors would like to thank the staff at the IRTF for their support during the observations. The Infrared Telescope Facility is operated by the University of Hawaii under Co-operative agreement no. NCC 5-538 with the National Aeronautics and Space Administration, Science Mission Directorate, Planetary Aeronomy Program. The authors are also grateful to the Open CLASTER project for the use of the RSTAR (a system for the transfer of atmospheric radiation) package in this research. This research is partly supported by Grant-in-aid for scientific research (C) no. 21540460 from the Ministry of Education, Culture, Sports, Science and Technology, Japan. SR acknowledges funding from by the Belgian Federal Science Policy Office (Action 1-MO/35/030) and would like to thank the IUAP PlanetTOPERS and EuroVenus (GA 606798) projects for their support

References

Bezard, B., Baluteau, J.-P., Marten, A., Coron, N., 1987. The $^{12}C/^{13}C$ and $^{16}O/^{18}O$ ratios in the atmosphere of Venus from high-resolution 10-μm spectroscopy. Icarus 72, 623–634.

Borkov, Y.u.G., Jacquemart, D., Lyulin, O.M., Tashkun, S.A., Perevalov, V.I., 2014. Infrared spectroscopy of ^{17}O- and ^{18}O-enriched carbon dioxide: Line positions and intensities in the 3200–4700 cm-1 region. Global modeling of the line positions of 16O12C17O and 17O12C17O. J. Quant. Spectrosc. Radiat. Transf. 137, 57–76.

Coplen, T.B., Bohlke, J.K., de Bievre, P., Ding, T., Holden, N.E., Hopple, J.A., Krouse, H. R., Lamberty, A., Peiser, H.S., Revesz, K., Rieder, S.E., Rosman, K.J.R., Roth, E., Taylor, P.D.P., Vocke, R.D., Xiao, Y.K., 2002. Isotope-abundance variations of selected elements. Pure Appl. Chem. 74 (1987–2017).

Donahue, T.M., Grinspoon, D.H., Heartle, R.E., Hodges Jr., R.R., 1997. (Venus II). In: Bougher, S.W., Hunten, D.M., Phillips, R.J. (Eds.), Ion/neutral escape of hydrogen and deuterium: Evolution of water. University of Arizona Press, Tucson, pp. 385–414.

Greene, T.P., Tokunaga, A.T., Toomey, D.W., Carr, J.B., 1993. CSHELL: A high spectral resolution 1–5 μm cryogenic Echelle spectrograph for the IRTF. Proc. SPIE 1946, 313–323.

Hoffman, J.H., Hodges, R.R., Donahue, T.M., McElroy, M.B., 1980. Composition of the Venus lower atmosphere from the Pioneer Venus mass spectrometer. J. Geophys. Res. 85, 7882–7890.

Humlicek, J., 1982. Optimized computation of the Voigt and complex probability functions. J. Quant. Spectrosc. Radiat. Transf. 27, 437–444.

Livingston, W., Wallace, L., 1991. An Atlas of the Solar Spectrum in the Infrared From 1850 to 9000 cm^{-1} (1.1 to 5.4 μm), N.S.O. Technical Report #91-001. National Solar Observatory, National Optical Astronomy Observatories, USA, pp. 67–107.

McKeegan, et al., 2011. The oxygen isotopic composition of the sun inferred from captured solar wind. Science 332, 1528–1532.

Nakajima, T., Tanaka, M., 1986. Matrix formulation for the transfer of solar radiation in a plane-parallel scattering atmosphere. J. Quant. Spectrosc. Radiat. Transf. 35, 13–21.

Nakajima, T., Tanaka, M., 1988. Algorithms for radiative intensity calculations in moderately thick atmospheres using a truncation approximation. J. Quant. Spectrosc. Radiat. Transf. 40, 51–69.

Picone, J.M., Hedin, A.E., Drob, D.P., Aikin, A.C., 2002. NRLMSISE-00 empirical model of the atmosphere: statistical comparisons and scientific issues. J. Geophys. Res. 107, 1468.

Pollack, J.B., Dalton, B., Grinspoon, D., Wattson, R.B., Freedman, R., Crisp, D., Allen, A., Bezard, B., de Bergh, C., Giver, L.P., Ma, Q., Tipping, R., 1993. Near-infrared light from Venus' nightside: A spectroscopic analysis. Icarus 103, 1–42.

Rothman, L....S., et al., 2013. The HITRAN 2012 molecular spectroscopic database. J. Quant. Spectrosc. Radiat. Transf. 130, 4–50.

Scott, E.R.D., 2001. Oxygen isotope give clues to the formation of planets, moons and asteroids. Planet. Sci. Discov. ⟨http://www.psrd.hawaii.edu/Dec01/Oisotopes.html/⟩.

Seiff, A., Schofield, J.T., Kliore, A.J., Taylor, F.W., Limaye, S.S., Rivercomb, H.E., Sromovsky, L.A., Kerzhanovich, V.V., Moroz, V.I., Marov, M.Y.a., 1985. Models of the structure of the atmosphere of Venus from the surface to 100 km altitude. Adv. Space Res. 5 (11), 3–58.

Takagi, S., Iwagami, N., 2011. Contrast source for the infrared images taken by the Venus mission AKATSUKI. Earth Planet Space 63, 435–442.

Thiemens, M.H., 1999. Mass-independent isotope effects in planetary atmosphere and the early solar system. Science 283, 341–345.